

# Isothermal Drying Characteristics and Kinetic Mechanism for Tobacco with Different Water Content

Wenfeng Liu,<sup>a</sup> Mei Chen,<sup>b</sup> Hui Liu,<sup>a</sup> Baojun Yi,<sup>b</sup> Hongyun Hu,<sup>c</sup> Yaohua Zhang,<sup>a</sup> Deqiang Liu,<sup>a</sup> and Chenqiao Li<sup>a,\*</sup>

The effect of drying temperature on the drying characteristics of tobacco was investigated with different water content. The isothermal drying characteristics and kinetics of three kinds of tobacco on the production line of a tobacco factory in Hubei were studied by halogen water analyzer. The drying characteristics of tobacco with different water content under isothermal conditions were evaluated by water loss characteristics, water diffusion coefficient, and activation energy. The results showed that the drying time of cut tobacco was reduced by increasing the drying temperature within a certain range. The water diffusion coefficient of cut tobacco decreased with the increase of temperature from 70 to 100 °C, and increased with the increase of initial water content. The activation energy of cut tobacco was related to the production process. The activation energy in the experiment was as follows: CT-2 > CT-3 > CT-1. Five drying models were used for non-linear fitting of the drying behavior of tobacco. The fitting degree of the Midilli model was the highest, reaching 0.9944. This data will be useful in the design of tobacco drying equipment.

DOI: 10.15376/biores.18.2.2611-2625

Keywords: Tobacco; Drying characteristics; Water diffusion coefficient; Activation energy

Contact information: a: China Tobacco Hubei Industry Co. Ltd, Wuhan 430052, P. R. China; b: School of Engineering, Huazhong Agricultural University, Wuhan 430040, P. R. China; c: School of Energy and Power Engineering, Huazhong University of Science and Technology, Wuhan 430074, P. R. China;

\* Corresponding author: lichenqiao@hbtobacco.cn

## INTRODUCTION

Tobacco drying is a complex process of heat and mass transfer (Bialik *et al.* 2020). The water content affects the aroma components, taste, and quality of finished tobacco (Xin *et al.* 2018). Drying (<100 °C) is the first stage of the heating process of tobacco. As the evaporation of water increases the resistance of heat and mass transfer in tobacco, this stage influences the temperature field distribution, total flue gas emission, and consistency in tobacco. Therefore, research on this process involves analysis of heat and mass transfer in cut tobacco, with emphasis on improving the quality of cigarette products.

The existing research mainly has focused on the impact of specific drying methods on the parameters of cigarette products, and there has been little research on the water content of tobacco directly. Zhu *et al.* (2015) studied the effects of radiation heat transfer conditions and vacuum on drying kinetics and temperature of tobacco leaves. Fu *et al.* (2019) used low-temperature vacuum drying technology to explore its effect on tobacco water, the results showed that the aromatic components of cut tobacco with low-temperature vacuum drying were higher than those with conventional drum drying. Ling

*et al.* (2015) used solar energy to dry tobacco, showing that the drying rate was related to the drying temperature and wind speed, and the change of water content had little effect on the drying rate. Xu *et al.* (2015) investigated the change of pore size during tobacco drying using a small dryer. The results showed that the inner pore volume, leaf volume, pore size distribution, and pore morphology of tobacco were related to the drying method. However, the cited studies mainly have focused on the quality of cut tobacco before and after drying. The moisture migration law of cut tobacco during drying still is not clear, and this imposes limitations on understanding the drying process of cut tobacco.

The drying kinetics and the water migration mechanism have been evaluated by studying the change of water content and the relationship between water and other factors (Gomez-de la Cruz *et al.* 2015; Sadaka and Atungulu 2018). Zhao *et al.* (2016) studied the drying kinetics of coal under different drying methods; they found that the Midilli-Kucuk model can best simulate the dehydration process of lignite in all drying methods. Pin *et al.* (2009) researched the effects of drying temperature on the quality and drying kinetics of areca leaves and selected five thin-layer models. Some studies on biomass materials such as cellulose (Al Zaitone and Al-Zahrani 2021) and vegetables and fruits (Dubkova *et al.* 2002) also have dealt with drying kinetics. But studies carried out so far usually have used thermogravimetric analyzers to conduct isothermal kinetics experiments on different materials (Hu *et al.* 2020). Due to the particularity of tobacco drying, it will cause greater error and affect the accuracy of the experimental results. Tobacco drying requires special equipment and strict temperature control, such that the established drying mechanisms may not be fully applicable to tobacco drying. Therefore, the research on the drying mechanism of tobacco has important guiding value in the process of tobacco production.

Research completed up to this point has not included in-depth analysis of the drying mechanism and drying model of tobacco. The use of a model with large error may bring losses to the production of tobacco. To solve this problem, some improved experimental methods and drying models have been explored in this article. In order to avoid the experimental error caused by the heating and cooling stage of thermogravimetric analysis, in this paper, the drying characteristics of cut tobacco were studied with a halogen water analyzer. On this basis, the effective diffusion coefficient and activation energy in the drying process of cut tobacco were calculated according to drying kinetics. Through the comparison of 5 drying models, the model with the highest fitting degree was selected, which was beneficial to evaluate the drying level of cut tobacco and had high guiding value for the production of cut tobacco.

## EXPERIMENTAL

### Materials

The cut tobacco was chosen from three kinds of cut tobacco with different grades (denoted as CT-1, CT-2, and CT-3) on the production line of a cigarette factory. For each grade, 200 g was dried in hot air at 55 °C until the mass change in 2 h was less than 1% to exclude the influence of initial water content. The tobacco samples used in the experiment were flakes with a thickness of about 0.3 mm, thus ensuring that they have sufficient contact and absorption of moisture. The water content was tested by HC103 halogen water meter (Metler-Toledo Instrument Co., Ltd., Shanghai, China) with 96 mm diameters of aluminum foil plate.

## Methods

During the pretreatment process, the moisture of tobacco was completely excluded, and 16%, 21%, 26%, and 31% moisture was added dropwise to the completely dry samples. Then the samples were maintained for 96 h in a closed environment at 22 °C, so that the moisture diffused evenly in the tobacco. The HC103 halogen water meter was adjusted to the target temperature (70 to 120 °C), and the cut tobacco samples with different water contents were dried at the target temperature. Each time, 3 g of cut tobacco raw materials were added and then placed into the aluminum foil plate of the halogen water meter for drying. The thickness of the cut tobacco layer was approximately 5 mm, and the drying stopped after the water content was constant within 50 s. Each sample was tested in triplicate to reduce errors.

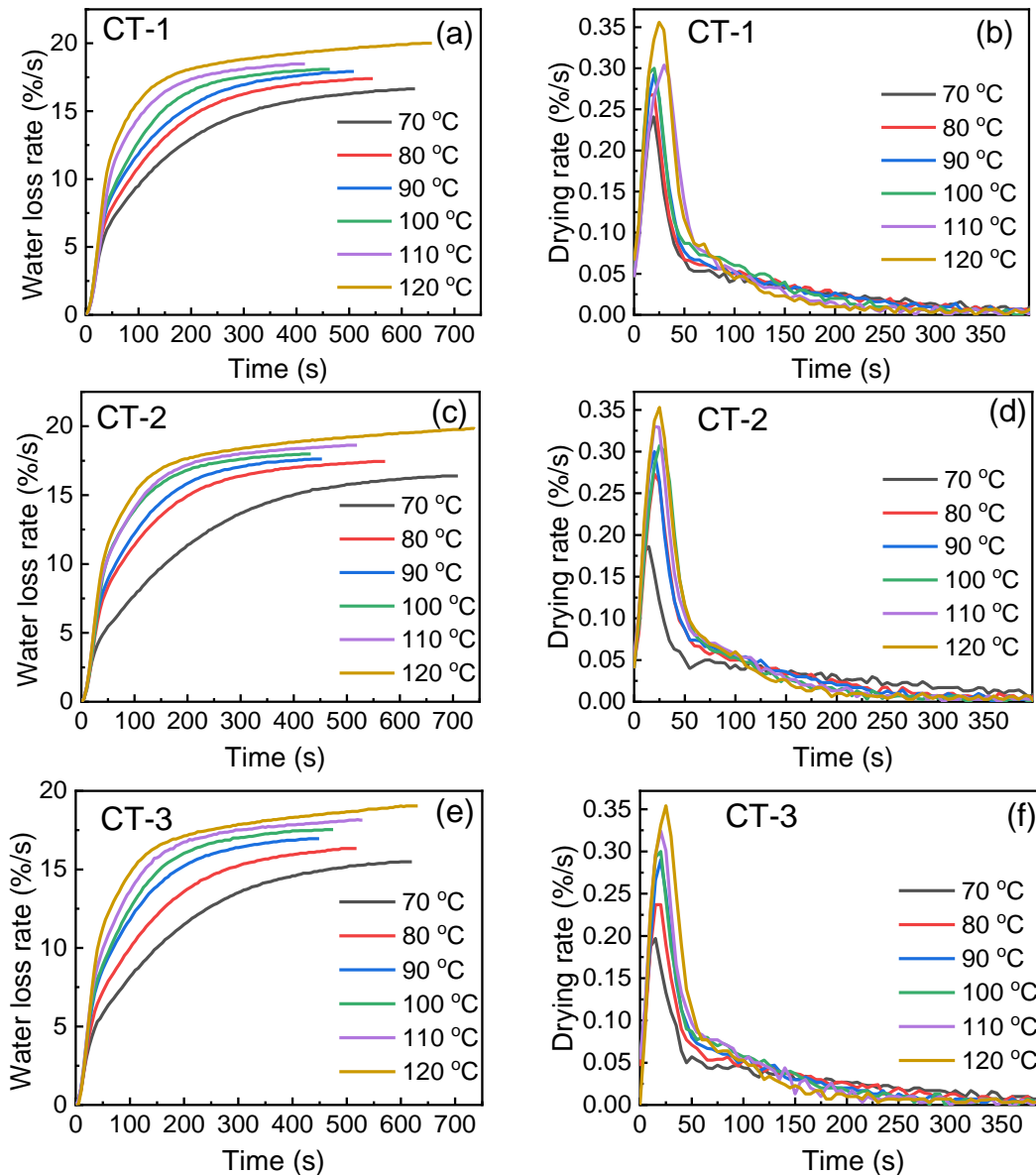
## RESULTS AND DISCUSSION

### Effect of Temperature on Drying of Tobacco

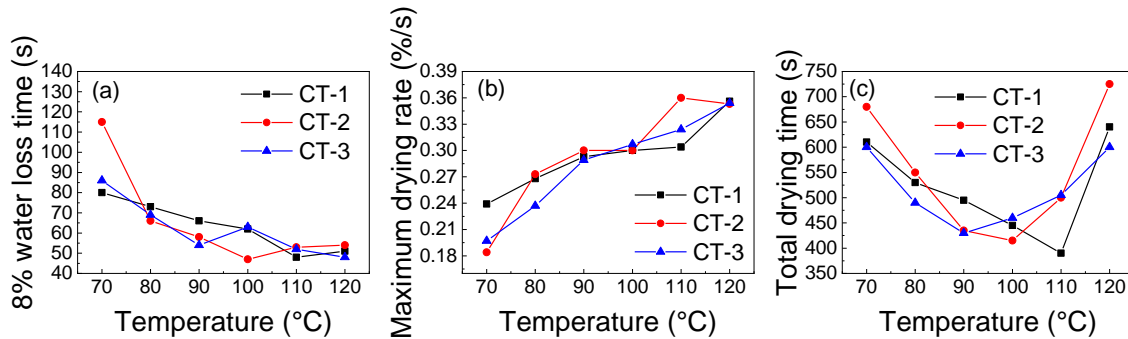
The dehydration rate and drying rate of three kinds of tobacco at different temperatures are shown in Fig. 1. The drying process of tobacco in a halogen water meter can be divided into three periods: a rising rate period, a first falling rate period, and a second falling rate period. In the rising rate period, with the increase of temperature, the drying curve was steeper, so the time required for the sample to reach the same water content was shorter. The reason is that a high drying temperature not only can increase the heat transfer rate and increase the evaporation rate of water on the surface of the tobacco, but also it can reduce the relative humidity of the drying indoor air and increase the diffusion power of the surface water of the sample to the air, which is similar to the drying process of coal or biomass. In the first falling rate period, the drying rate decreased rapidly in a short time, which was mainly caused by the loss of non-binding water inside the tobacco (Sahoo *et al.* 2022). In the rising rate period and the first falling rate period, the change of drying rate with temperature was more obvious. In the early stage of drying, there is more non-binding water in the tobacco, and the rate of internal water to the surface of the tobacco is close to the evaporation rate of water from the surface of the tobacco. At this time, the diffusion process of water is greatly affected by heating temperature. After entering the second falling rate period, the content of non-bound water decreases, and the rate of water diffusion to the surface of tobacco is less than the evaporation rate of water on the surface of tobacco, so the drying time is less affected by temperature.

Figure 2 shows the variation of water loss rate, total drying time, and maximum drying rate of the three kinds of cut tobacco with temperature. Figure 2(a) shows that the drying rate of cut tobacco continued to increase with the increase of temperature. In the range of 80 to 100 °C, with the increase of drying temperature, the time for water content of cut tobacco to reach 8% was gradually shortened, and the total drying time of three cut tobacco gradually decreased with the increase of temperature, and it suddenly increased after 100 °C (Fig. 2b, c). The evaporation pressure difference of free water inside cut tobacco increased with increasing drying temperature, thereby reducing drying time. However, the temperature higher than 100 °C can affect free water and bound water in cut tobacco at the same time, and some bound water is converted to free water. Therefore, a longer drying time is needed (Velaga *et al.* 2018). In addition, the content of alcohol

compounds is often more than 10% (e.g., ethyl alcohol, glycerol, etc.). When the temperature is above 100 °C, such substances also have a tendency to volatilize, so the drying time will be prolonged for the obvious. Therefore, the drying temperature of cut tobacco is an important factor affecting the drying time of cut tobacco. According to different production processes of cut tobacco, the drying temperature at 90 to 100 °C improved the drying efficiency. When the drying temperature continues to increase, it not only prolongs the drying time of tobacco, but it also leads to the loss of potential components in tobacco and reduces the quality of tobacco.



**Fig. 1.** Changes of water loss rate and drying rate with time of three kinds of cut tobacco at different temperatures. (a) CT-1, water loss rate; (b) CT-1, drying rate; (c) CT-2, water loss rate; (d) CT-2, drying rate; (e) CT-3, water loss rate; (f) CT-3, drying rate



**Fig. 2.** Changes of dehydration rate, total drying time and maximum drying rate of three kinds of tobacco with temperature. (a) Maximum drying rate; (b) The water loss rate reached 8%; (c) Total drying time

### Effect of Initial Water Content on Drying of Tobacco

The hot air-drying method was used to dry the cut tobacco with different initial water contents (5% gradients). The water loss rates in different time periods are shown in Fig. 3. Within 50 s of drying, the cut tobacco with different water contents had similar water loss trends. With increasing time, the water loss rate of cut tobacco gradually slowed down, and it tended to be stable after 400 s. This was because in the early stage of drying, the internal water diffusion rate of cut tobacco was much larger than the surface water evaporation rate, and the internal water diffusion rate gradually decreased so that it could not meet the surface evaporation, leading to the decrease of drying rate and the smooth drying curve (Sojak and Glowacki 2010). The increasing of the initial moisture content of tobacco will increase its maximum water loss rate. In addition, compared with CT-2, the difference of several curves of CT-1 was not uniform in the stable stage, which means that no matter the length of drying time, some water cannot be lost at this temperature. This phenomenon is related to the production process of cut tobacco. The drying rate was positively correlated with the initial water content. The drying rate reached the peak in the initial 50 s, and then it decreased. Under different initial water content, there was little difference in the slope between the rising stage and the first deceleration stage, and the slope of the second deceleration stage changed more obviously. These results indicated that the initial water content of tobacco had a great influence on the second deceleration stage, but it had no obvious impact on the rising and the first deceleration period.

### Determination of Effective Diffusion Coefficient of Water

The diffusion coefficient reflects the dehydration ability of the material under certain drying conditions. Convection drying of tobacco contains complex heat and mass transfer process, in which the heat and mass coupling, the spatial distribution, and the internal microstructure of tobacco make the diffusion of internal water present a complex state. In the dynamic study, the drying process of cut tobacco was simplified as a separate study of the drying characteristics of cut tobacco, and assumptions were made (Pathare and Sharma 2006): (1) The internal isotropic and uniform structure distribution of cut tobacco, the internal temperature difference was negligible; (2) The thermal and mass coupling effects in the drying process were ignored; (3) The size of cut tobacco was calculated with average size, and the deformation during drying was ignored; and (4) Water migration during drying conforms to Fick's diffusion law.

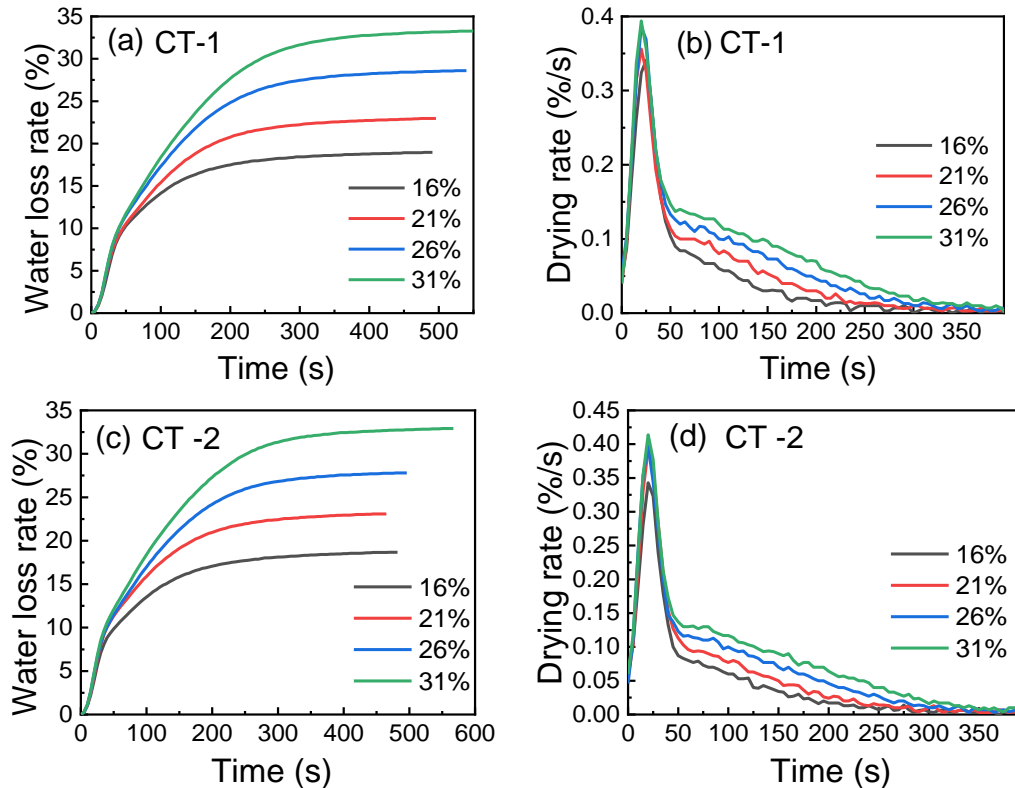


**Fig. 3.** Changes of dehydration rate and drying rate with time under different initial water content at 100 °C. (a) CT-1, Water loss rate; (b) CT-1, Drying rate; (c) CT-2, Water loss rate; (d) CT-2, Drying rate

Equation 1 is the expression of Fick's second law, and Eq. 2 is the expression when higher-order terms are ignored. The solution of the water diffusion coefficient is based on the following assumptions: The change of volume and size of materials during drying can be ignored; in the initial state, the moisture and temperature inside the material are evenly distributed, and the temperature is consistent with the ambient temperature; and the moisture inside the material diffuses in one dimension on an infinite plate. The evaporation of water only occurs on the surface of the material. The material is heat conduction inside and convective heat transfer outside. The effective moisture diffusion coefficient is taken to be a constant (Zafer and Filiz 2010; Vega-Galvez *et al.* 2010; Deng *et al.* 2017).

Equation 3 shows that the natural logarithm of water ratio  $\ln MR$  during drying is linear with drying time  $t$ . The quantity  $\ln MR$  gradually decreases with time. The slope  $k$  is obtained by linear fitting of the curve, and the water diffusion coefficient  $D_{eff}$  is calculated by Eq. 3, as follows,

$$\frac{\partial MR}{\partial t} = \nabla[D_{eff}(\nabla MR)] \quad (1)$$

$$MR = \frac{8}{\pi^2} \sum_{n=0}^{\infty} \frac{1}{(2n+1)^2} \exp\left(-\frac{(2n+1)^2 \pi^2 D_{eff} t}{4L^2}\right) \quad (2)$$

$$\ln MR = \ln \frac{8}{\pi^2} - \frac{\pi^2 D_{eff}}{4\delta^2} t \quad (3)$$

where  $MR$  is the water ratio,  $D_{eff}$  is the water diffusion coefficient ( $m^2 s^{-1}$ ),  $t$  is time (s), and  $\delta$  is the dry thickness (mm).

The water diffusion coefficients of three tobacco samples at various drying temperatures are shown in Fig. 4 (a). When the heating temperature was 70 to 100 °C, the water diffusion coefficient of CT-1 was  $0.8703 \times 10^{-7}$  to  $1.3121 \times 10^{-7} \text{ m}^2 \text{ s}^{-1}$ . The water diffusion coefficient of CT-2 was  $0.7852 \times 10^{-7}$  to  $1.4154 \times 10^{-7} \text{ m}^2 \text{ s}^{-1}$ , and the water diffusion coefficient of CT-3 was  $0.8896 \times 10^{-7}$  to  $1.2999 \times 10^{-7} \text{ m}^2 \text{ s}^{-1}$ . In the temperature range of 70 to 100 °C, the water diffusion coefficient values of first, second, and third tobacco increased with the increased temperature. With increased drying temperature, the energy of water molecules in tobacco increased, and the increased transition frequency led to the increase of transition distance of water molecules, which led to the increase of diffusion coefficient of tobacco with the increase of temperature. When the temperature was higher than 100 °C, the evaporation of water was easier, and the aggregation of water vapor on the surface of tobacco would affect the continued diffusion of internal water. At this temperature, the conversion of bound water to free water also reduced the water diffusion coefficient. In addition, high temperature can lead to the loss of chemical components such as glycerol in tobacco, which also can affect the water diffusion coefficient.

Figure 4(b-c) shows the change of water diffusion coefficient of tobacco under different initial water content. The water diffusion coefficient of tobacco increased with the increase of temperature from 70 °C to 100 °C under different initial water, which is consistent with the law of the original sample. When the first and second cut tobaccos were at 70 to 100 °C, the water diffusion coefficient of cut tobaccos generally decreased with the increase of initial water content. The higher initial water content of tobacco resulted in a higher non-binding water content of tobacco, resulting in the water diffusion coefficient decreasing with initial water content in a certain temperature range (Torki-Harchegani *et al.* 2016). Under drying conditions of 110 °C and 120 °C, the water diffusion coefficient of tobacco changed with initial water content. When the drying temperature exceeds 100 °C, water is evaporated directly from inside of tobacco in the form of gas. The rapid collision of water vapor molecules with tobacco leads to a spatial residence, which leads to the emergence of spatial water vapor (Torki-Harchegani *et al.* 2016). At the same time, the bound water in tobacco is gradually released at this temperature, resulting in a higher temperature and lower water diffusion coefficient.

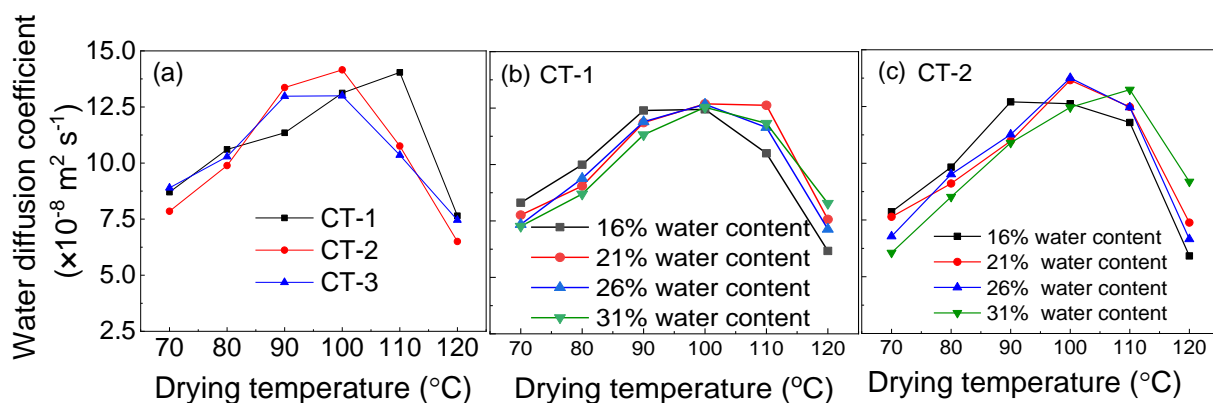


**Fig. 4.** The variation of water diffusion coefficient of three kinds of raw tobacco and tobacco with different initial water content. (a) Different tobacco; (b) CT-1, different initial water content; (c) CT-2, different initial water content



## Activation Energy

Drying activation energy refers to energy required by the target material to remove water per unit mass. A larger calculated activation energy indicates greater drying difficulty. The relationship between activation energy and water diffusion coefficient is obtained by the evolution of Arrhenius formula, as shown in Eq. 4.

$$\ln D_{eff} = \ln D_0 - \frac{E_a}{R} \frac{1}{T+273.15} \quad (4)$$

According to Eq. 4, if the natural logarithm of effective diffusion coefficient  $\ln D_{eff}$  and Calvin reciprocal  $1/(T+273.15)$  are linearly related, then the activation energy of tobacco can be calculated by the slope. Figure 5 (b) is the change of activation energy of CT-1 and CT-2 with initial moisture content under different moisture content. The activation energies of cut tobacco increase with the increase of the initial moisture content. It is because the increase of initial water content leads to more water needed to dry, so that caused more energy. In addition, with the increase of moisture content, the increment of activation energy decreases, which means that the drying of tobacco has a higher economic value under higher moisture content. Taking CT-1 as an example, when the moisture content increases from 26% to 31%, the activation energy required for drying increases only by 1.2%. The activation energy of tobacco itself was also tested. The results showed that the activation energies of the three kinds of tobacco were 13.85, 22.12, and 14.92 kJ/mol, respectively, indicating that the activation energy of tobacco was determined by the quality of tobacco and the production process. On this basis, an appropriate production process will be conducive to reducing the drying cost of tobacco.

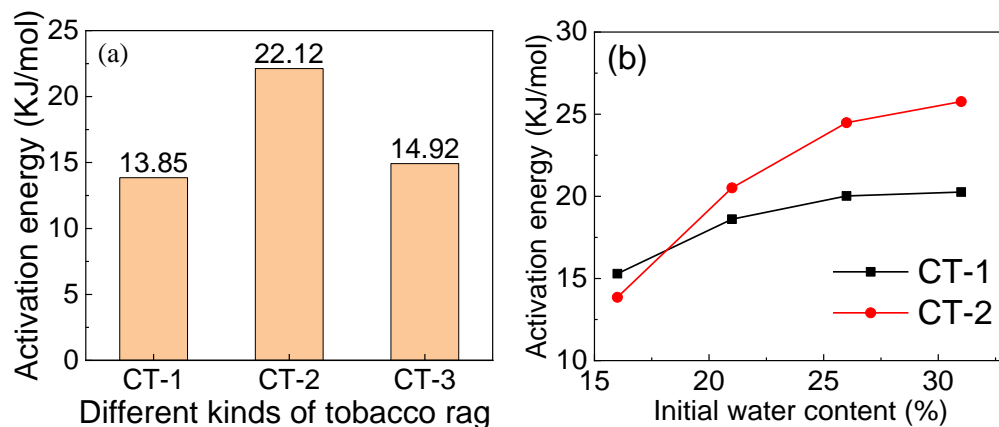


**Fig. 5.** The activation energy of tobacco and its influence by initial water content. (a) different tobacco; (b) different initial water content

## Model Fitting

The five common drying models in Table 1 were used to nonlinearly fit the water ratios of three original tobacco samples with time. The determination coefficient  $R^2$  was used to evaluate the fitting results (Sahoo *et al.* 2022). This value is used for quantitative comparison and shows the consistency level between the experimental data and the calculated data (Erbay and Icier 2010). The parameter  $x^2$  is the deviation between the experimental value and the predicted value of the model. A lower value indicates a better fit. The optimal model is selected by combining the two parameters.



**Table 1.** Mathematical Model for Drying Thin Layer of Tobacco

No.	Model	Expression	Coefficient	Reference
1	Newton (Lewis)	$MR = \exp(-kt)$	$k$	(El-Beltagy <i>et al.</i> 2007)
2	Page	$MR = \exp(-kt^n)$	$k, n$	(Jamaluddin <i>et al.</i> 2022)
3	Midilli	$MR = a \exp[(-kt)^n] + bt$	$a, b, k, t$	(Hu <i>et al.</i> 2009)
4	Logarithmic	$MR = a \times \exp(-kt) + c$	$a, b, k_0, k_1$	(Zheng <i>et al.</i> 2014)
5	Henderson and Pabis	$MR = a \exp(-kt)$	$a, k$	(Gornicki and Kaleta 2007)

The fitting parameters for each model are shown in Table 2. At 70 to 100 °C, the  $R^2$  values of the tobacco-Newton, Page, Middili, Logarithmic, and Henderson models were greater than 0.9777, 0.9928, 0.9944, 0.9862, and 0.9681, respectively. Comparing the  $X$  value of the Middili and Page models, the  $x^2$  value of tobacco-Page was lower than  $3.72 \times 10^{-4}$ , and the Middili value was lower than  $2.95 \times 10^{-4}$  at 70 to 100 °C. Therefore, the fitting value of Middili model was closer to the experimental value. Similarly, CT-2 and CT-3 achieved the best fit with the Middili model. At temperatures above 100 °C, the  $k$  value fluctuated to varying degrees, because 100 °C was the critical point for the transformation of water from liquid to gas. The gasification process is an endothermic reaction, which will lead to a sudden decrease in the local temperature of tobacco, and then lead to the fluctuation of the  $k$  value.

## CONCLUSIONS

1. The drying temperature is an important factor affecting the drying of cut tobacco. Increasing the drying temperature within a certain range could reduce the drying time of cut tobacco and reduce the drying cost of tobacco. But when the temperature exceeds 100 °C, the precipitation of bound water and other chemical components will be released. At this point, high drying temperature will lead to higher cost, and it will affect the tobacco fragrance effect. Therefore, the actual drying temperature should not exceed 100 °C in industrial drying.
2. Through the nonlinear fitting of the natural logarithm and time of the water ratio of tobacco, the water diffusion coefficient was calculated and its synergistic relationship with temperature was studied. The water diffusion coefficient was negatively correlated with temperature and positively correlated with initial water content at 70 to 100 °C. In addition, this research found that the drying of cut tobacco with high initial moisture content had higher economic benefits, and the activation energy of tobacco was related to the production process. These results shown that the initial moisture content of tobacco can be adjusted by optimizing the production process to reduce the drying cost.
3. By comparing the five different drying models, it was found that the tobacco produced by different processes could achieve better fitting when using the Midilli model, and a higher  $R^2$  ( $> 0.9944$ ) was obtained, indicating that the Midilli model could well describe the diffusion process of water in tobacco. In actual production, the drying situation of tobacco could be predicted based on the Midilli model, which is expected to be conducive to improving the yield of tobacco.

**Table 2.** Fitting Results of Drying Model of Cut Tobacco

Model	Temp. (°C)	CT-1			CT-2			CT-3		
		Model Parameter	R <sup>2</sup>	$\chi^2$	Model Parameter	R <sup>2</sup>	$\chi^2$	Model Parameter	R <sup>2</sup>	$\chi^2$
Newton	70	k=0.0092	0.978	11×10 <sup>-4</sup>	k=0.0092	0.977	12×10 <sup>-4</sup>	k=0.0080	0.983	9.3×10 <sup>-4</sup>
	80	k=0.0111	0.983	8.67×10 <sup>-4</sup>	k=0.0111	0.985	7.31×10 <sup>-4</sup>	k=0.0106	0.986	8.00×10 <sup>-4</sup>
	90	k=0.0124	0.981	9.96×10 <sup>-4</sup>	k=0.0124	0.978	9.50×10 <sup>-4</sup>	k=0.0137	0.988	6.74×10 <sup>-4</sup>
	100	k=0.0142	0.992	4.55×10 <sup>-4</sup>	k=0.0142	0.992	4.75×10 <sup>-4</sup>	k=0.0144	0.992	4.40×10 <sup>-4</sup>
	110	k=0.0169	0.988	7.04×10 <sup>-4</sup>	k=0.0169	0.988	7.58×10 <sup>-4</sup>	k=0.0159	0.988	5.74×10 <sup>-4</sup>
	120	k=0.0172	0.968	12×10 <sup>-4</sup>	k=0.0172	0.968	12×10 <sup>-4</sup>	k=0.0166	0.965	14×10 <sup>-4</sup>
Page	70	k=0.0236 n=0.810	0.998	2.67×10 <sup>-4</sup>	k=0.0237 n=0.809	0.995	2.69×10 <sup>-4</sup>	k=0.0176 n=0.846	0.994	3.23×10 <sup>-4</sup>
	80	k=0.0242 n=0.836	0.995	2.82×10 <sup>-4</sup>	k=0.0242 n=0.836	0.995	2.35×10 <sup>-4</sup>	k=0.0215 n=0.853	0.995	2.83×10 <sup>-4</sup>
	90	k=0.0272 n=0.830	0.993	3.72×10 <sup>-4</sup>	k=0.0272 n=0.830	0.992	3.55×10 <sup>-4</sup>	k=0.0239 n=0.878	0.994	3.64×10 <sup>-4</sup>
	100	k=0.0218 n=0.904	0.995	2.90×10 <sup>-4</sup>	k=0.0219 n=0.903	0.995	3.02×10 <sup>-4</sup>	k=0.0224 n=0.901	0.995	2.70×10 <sup>-4</sup>
	110	k=0.0150 n=1.029	0.988	7.07×10 <sup>-4</sup>	k=0.0155 n=1.021	0.988	7.61×10 <sup>-4</sup>	k=0.0257 n=0.889	0.992	4.05×10 <sup>-4</sup>
	120	k=0.0334 n=0.840	0.975	9.57×10 <sup>-4</sup>	k=0.0342 n=0.835	0.974	9.86×10 <sup>-4</sup>	k=0.0347 n=0.825	0.973	11×10 <sup>-4</sup>
Midilli	70	a=1.049 k=0.0361 n=0.726 b=- 4.356×10 <sup>-5</sup>	0.997	1.81×10 <sup>-4</sup>	a=1.0493 k=0.0363 n=0.725 b=- 4.487×10 <sup>-5</sup>	0.997	1.85×10 <sup>-4</sup>	a=1.0191 k=0.0272 n=0.751 b=- 7.895×10 <sup>-5</sup>	0.997	1.50×10 <sup>-4</sup>
	80	a=1.052 k=0.0354 n=0.761 b=- 3.457×10 <sup>-5</sup>	0.996	2.17×10 <sup>-4</sup>	a=1.0466 k=0.0329 n=0.728 b=- 1.706×10 <sup>-5</sup>	0.996	1.97×10 <sup>-4</sup>	a=1.0488 k=0.0324 n=0.770 b=- 4.977×10 <sup>-5</sup>	0.996	2.08×10 <sup>-4</sup>
	90	a=1.066 k=0.0401 n=0.755 b=- 2.676×10 <sup>-5</sup>	0.994	2.95×10 <sup>-4</sup>	a=1.272 k=0.0860 n=0.619 b=- 5.173×10 <sup>-5</sup>	0.997	1.37×10 <sup>-4</sup>	a=1.0624 k=0.0338 n=0.811 b=- 1.820×10 <sup>-5</sup>	0.995	2.93×10 <sup>-4</sup>

	100	a=1.058 k=0.0300 n=0.844 b=- 8.376×10 <sup>-6</sup>	0.996	2.33×10 <sup>-4</sup>		a=1.0580 k=0.0300 n=0.8450 b=- 7.56×10 <sup>-6</sup>	0.996	2.43×10 <sup>-4</sup>		a=1.0564 k=0.0299 n=0.848 b=- 3.728×10 <sup>-6</sup>	0.994	2.15×10 <sup>-4</sup>
	110	a=1.078 k=0.0212 n=0.968 b=- 3.064×10 <sup>-5</sup>	0.992	5.14×10 <sup>-4</sup>		a=1.0760 k=0.0205 n=0.977 b=- 4.20×10 <sup>-5</sup>	0.992	5.37×10 <sup>-4</sup>		a=1.0709 k=0.0328 n=0.850 b=- 2.322×10 <sup>-5</sup>	0.995	2.74×10 <sup>-4</sup>
	120	a=1.106 k=0.0442 n=0.802 b=- 3.399×10 <sup>-5</sup>	0.983	6.54×10 <sup>-4</sup>		a=1.102 k=0.0424 n=0.811 b=- 3.867×10 <sup>-5</sup>	0.983	6.57×10 <sup>-4</sup>		a=1.1096 k=0.0427 n=0.806 b=- 4.683×10 <sup>-5</sup>	0.983	7.18×10 <sup>-4</sup>
Logarithmic	70	a=0.902 k=0.0087 c=- 0.0133	0.988	6.34×10 <sup>-4</sup>		a=0.902 k=0.0088 c=- 0.0147	0.988	6.42×10 <sup>-4</sup>		a=0.909 k=0.0072 c=-0.0015	0.992	4.57×10 <sup>-4</sup>
	80	a=0.927 k=0.0108 c=- 0.0122	0.989	5.89×10 <sup>-4</sup>		a=0.927 k=0.0107 c=- 0.0093	0.990	4.99×10 <sup>-4</sup>		a=0.934 k=0.0104 c=-0.0126	0.990	5.49×10 <sup>-4</sup>
	90	a=0.936 k=0.0124 c=- 0.0175	0.986	7.21×10 <sup>-4</sup>		a=0.921 k=0.0120 c=- 0.0137	0.985	6.68×10 <sup>-4</sup>		a=0.967 k=0.0142 c=- 0.0164	0.991	5.46×10 <sup>-4</sup>
	100	a=0.980 k=0.0146 c=- 0.0116	0.993	3.94×10 <sup>-4</sup>		a=0.980 k=0.0147 c=- 0.0130	0.993	4.04×10 <sup>-4</sup>		a=0.980 k=0.0149 c=-0.0130	0.993	3.64×10 <sup>-4</sup>
	110	a=1.058 k=0.0190 c=- 0.0150	0.992	4.75×10 <sup>-4</sup>		a=1.0571 k=0.0192 c=- 0.0175	0.992	4.90×10 <sup>-4</sup>		a=0.994 k=0.0172 c=-0.0206	0.993	3.62×10 <sup>-4</sup>
	120	a=1.015 k=0.0200 c=- 0.0300	0.984	6.08×10 <sup>-4</sup>		a=1.0154 k=0.0201 c=- 0.0314	0.985	5.97×10 <sup>-4</sup>		a=1.016k=0 .0198 c=- 0.0357	0.984	6.65×10 <sup>-4</sup>
Henderson	70	a=0.902 k=0.0082	0.987	6.77×10 <sup>-4</sup>		a=0.902 k=0.0082	0.987	6.93×10 <sup>-4</sup>		a=0.909 k=0.0073	0.992	4.53×10 <sup>-4</sup>
	80	a=0.927 k=0.0102	0.988	6.31×10 <sup>-4</sup>		a=0.927 k=0.0102	0.989	5.30×10 <sup>-4</sup>		a=0.9345 k=0.0099	0.990	5.83×10 <sup>-4</sup>
	90	a=0.934 k=0.0115	0.984	8.18×10 <sup>-4</sup>		a=0.916 k=0.0112	0.984	7.27×10 <sup>-4</sup>		a=0.967 k=0.0133	0.989	6.30×10 <sup>-4</sup>

	100	a=0.981 k=0.0139	0.992	$4.44 \times 10^{-4}$		a=0.981 k=0.0139	0.992	$4.64 \times 10^{-4}$		a=0.980 k=0.0141	0.992	$4.28 \times 10^{-4}$
	110	a=1.0583 k=0.0180	0.990	$5.80 \times 10^{-4}$		a=1.0583 k=0.0180	0.990	$6.25 \times 10^{-4}$		a=0.992 k=0.0157	0.988	$5.77 \times 10^{-4}$
	120	a=1.0075 k=0.0173	0.968	$12 \times 10^{-4}$		a=1.0075 k=0.0173	0.968	$12 \times 10^{-4}$		a=1.0062k= 0.0167	0.965	$15 \times 10^{-4}$

## ACKNOWLEDGMENTS

This research was financially supported by the Hubei Province Key Research and development Program (2021BCA157) and the Supports Technological Innovation Development Project of Hubei Province (2021BAB115).

## REFERENCES CITED

- Al Zaitone, B., and Al-Zahrani, A. (2021). "Spray drying of cellulose nanofibers: Drying kinetics modeling of a single droplet and particle formation," *Chemical Engineering & Technology* 44(7), 1270-1277. DOI: 10.1002/ceat.202000579
- Bialik, M., Wiktor, A., Witrowa-Rajchert, D., Samborska, K., Gondek, E., and Findura, P. (2020). "Osmotic dehydration and freezing as a suitable pretreatment in the process of vacuum drying kiwiberry: Drying kinetics and microstructural changes," *International Agrophysics* 34(2), 265-272. DOI: 10.31545/intagr/118859
- Deng, L. Z., Yang, X. H., Mujumdar, A. S., Zhao, J. H., Wang, D., Zhang, Q., Wang, J. W., Gao, Z. J., and Xiao, H. W. (2017). "Red pepper drying: Effects of different drying methods on drying kinetics, physicochemical properties, antioxidant capacity, and microstructure," *Drying Technology* 36(8), 893-907. DOI: 10.1080/07373937.2017.1361439
- Dubkova, N. Z., Galiakberov, Z. K., and Nikolaev, N. A. (2002). "The research on kinetics of drying when making powder of vegetable raw materials," *Khranenie i Pererabotka Sel'khozsyrya*(No. 2), 30-34.
- El-Beltagy, A., Gamea, G. R., and Essa, A. H. A. (2007). "Solar drying characteristics of strawberry," *Journal of Food Engineering* 78(2), 456-464. DOI: 10.1016/j.jfoodeng.2005.10.015
- Erbay, Z., and Icier, F. (2010). "A review of thin layer drying of foods: Theory, modeling, and experimental results," *Critical Reviews in Food Science and Nutrition* 50(5), 441-464. DOI: 10.1080/10408390802437063
- Fu, L., Yi, B., Wen, Y., Li, W., Lin, W., Ma, N. I., Tang, J., Liu, Z., Zhou, B., and Gao, X. (2019). "Effects of low temperature vacuum drying on quality of cut tobacco and cigarette," *Acta Tabacaria Sinica* 25(3), 23-28.
- Gomez-de la Cruz, F. J., Casanova-Pelaez, P. J., Lopez-Garcia, R., and Cruz-Peragon, F. (2015). "Review of the drying kinetics of olive oil mill wastes: Biomass recovery," *BioResources* 10(3), 6055-6080. DOI: 10.15376/biores.10.3. 6055-6080
- Gornicki, K., and Kaleta, A. (2007). "Modelling convection drying of blanched parsley root slices," *Biosystems Engineering* 97(1), 51-59. DOI: 10.1016/j.biosystemseng.2007.02.006
- Hu, L., He, L., and Wang, G. (2020). "Drying kinetics characteristics of lignite using thermogravimetric analysis," *Energy Sources Part a-Recovery Utilization and Environmental Effects* 42(5), 586-596. DOI: 10.1080/15567036.2019.1587105
- Hu, Z., Wang, H., Xie, H., Wu, F., Chen, Y., and Cao, S. (2009). "Mathematical models and model predictive control for crossflow grain drying," *Transactions of the Chinese Society of Agricultural Engineering* 25(4), 96-102.

- Jamaluddin, Yahya, M., Rauf, R. F., and Rivai, A. A. (2022). "Drying kinetics and quality characteristics of *Eucheuma cottonii* seaweed in various drying methods," *Journal of Food Processing and Preservation* 46(2). DOI: 10.1111/jfpp.16258
- Ling, D., Li, M., Luo, X., Ji, X., Liu, J., Zhang, P., and Cai, W. (2015). "Study on drying characteristics of cut tobacco based on trough concentrating solar heating," *Acta Energetica Solaris Sinica* 36(2), 460-466.
- Pathare, P. B., and Sharma, G. P. (2006). "Effective moisture diffusivity of onion slices undergoing infrared convective drying," *Biosystems Engineering* 93(3), 285-291. DOI: 10.1016/j.biosystemseng.2005.12.010
- Pin, K. Y., Chuah, T. G., Rashih, A. A., Law, C. L., Rasadah, M. A., and Choong, T. S. Y. (2009). "Drying of betel leaves (*Piper betle* L.): Quality and drying kinetics," *Drying Technology* 27(1), 149-155. DOI: 10.1080/07373930802566077
- Sadaka, S., and Atungulu, G. (2018). "Grain sorghum drying kinetics under isothermal conditions using thermogravimetric analyzer," *BioResources* 13(1), 1534-1547. DOI: 10.15376/biores.13.1.1534-1547
- Sahoo, M., Titikshya, S., Aradwad, P., Kumar, V., and Naik, S. N. (2022). "Study of the drying behaviour and color kinetics of convective drying of yam (*Dioscorea hispida*) slices," *Industrial Crops and Products* 176. DOI: 10.1016/j.indcrop.2021.114258
- Sojak, M., and Glowacki, S. (2010). "Analysis of giant pumpkin (*Cucurbita maxima*) drying kinetics in various technologies of convective drying," *Journal of Food Engineering* 99(3), 323-329. DOI: 10.1016/j.jfoodeng.2010.03.010
- Torki-Harchegani, M., Ghasemi-Varnamkhasti, M., Ghanbarian, D., Sadeghi, M., and Tohidi, M. (2016). "Dehydration characteristics and mathematical modelling of lemon slices drying undergoing oven treatment," *Heat and Mass Transfer* 52(2), 281-289. DOI: 10.1007/s00231-015-1546-y
- Vega-G., A., Miranda, M., and Díaz, L. P. (2010). "Effective moisture diffusivity determination and mathematical modeling of the drying curves of the olive-waste cake," *Bioresource Technology* 101(19), 7265-7270. DOI: 10.1016/j.biortech.2010.04.040
- Velaga, S. P., Nikjoo, D., and Vuddanda, P. R. (2018). "Experimental studies and modeling of the drying kinetics of multicomponent polymer films," *Aaps Pharmscitech* 19(1), 425-435. DOI: 10.1208/s12249-017-0836-8
- Xin, Y. N., Zhang, J. W., and Li, B. (2018). "Drying kinetics of tobacco strips at different air temperatures and relative humidities," *Journal of Thermal Analysis and Calorimetry* 132(2), 1347-1358. DOI: 10.1007/s10973-018-7005-5
- Xu, B., Zhu, W., Pan, G., Shen, Y., Li, B., and Yu, C. (2015). "Variation of pore structure in cut strips dried by different drying means," *Tobacco Science and Technology* 48(4), 60-65.
- Zafer, E., and Filiz, I. (2010). "A review of thin layer dry of foods: Theory, modeling, and experimental results," *Critical Review in Food Science and Nutrition* 50(5), 441-464. DOI: 10.1080/10408390802437063
- Zhao, P. F., Zhong, L. P., Zhu, R., Zhao, Y. M., Luo, Z. F., and Yang, X. L. (2016). "Drying characteristics and kinetics of Shengli lignite using different drying methods," *Energy Conversion and Management* 120, 330-337. DOI: 10.1016/j.enconman.2016.04.105

- Zheng, Q.-y., Wang, D., Ma, Y., Zhao, X.-y., and Tong, J.-m. (2014). "Hot air drying characteristics and mathematical model of green pepper," *Food Industry* 12, 136-139.
- Zhu, W. K., Wang, L., Duan, K., Chen, L. Y., and Li, B. (2015). "Experimental and numerical investigation of the heat and mass transfer for cut tobacco during two-stage convective drying," *Drying Technology* 33(8), 907-914. DOI: 10.1080/07373937.2014.997882

Article submitted: May 18, 2022; Peer review completed: June 19, 2022; Revised version received and accepted: July 12, 2022; Published: February 6, 2023.  
DOI: 10.15376/biores.18.2.2611-2625